

Establishment of Type 2 Diabetes Mellitus Models Using High-Fat Diet and STZ in Bama Minipigs

Yuqiong Zhao

Chinese PLA General Hospital

Miaomiao Niu

Chinese PLA General Hospital

Jia Yunxiao

PLAGH: Chinese PLA General Hospital

Yuan Jifang

Chinese PLA General Hospital

Xiang Lei

Laboratory Animal Center, Chinese PLA General Hospital

Dai Xin

Chinese PLA General Hospital

Wang Guisheng

Radiology Department of No.3 Clinical Center, Chinese PLA General Hospital

Hua Chen (✉ chenhua301paper@163.com)

Chinese PLA General Hospital <https://orcid.org/0000-0003-0110-2933>

Research Article

Keywords: type 2 diabetes, atherosclerosis, streptozotocin, miniature swine, beta cell activity

Posted Date: September 30th, 2021

DOI: <https://doi.org/10.21203/rs.3.rs-602880/v1>

License:  This work is licensed under a Creative Commons Attribution 4.0 International License.

[Read Full License](#)

Abstract

Background

In the past 20 years, the number of adults with diabetes has tripled. For most of the researches are often conducted in rodent T2DM models, and effective drugs developed have low clinical conversion efficiency. Therefore, it is urgent to establish a large animal model to explore the pathogenesis of T2DM and formulate disease prevention and control strategies.

Methods

This study was designed to establish and validate a T2DM model in minipigs with notable hyperglycemia using a high-fat diet and low-dose streptozotocin (STZ) and examined the influence of STZ infusion time, the difference between a high-fat diet and a high-cholesterol and high-fat diet, and the atherosclerotic lesions accelerated by diabetes. Male Bama minipigs (n=24) were randomly divided into 5 groups; the control group was fed with normal diet for 9 months; STZ+HFD group and STZ+HCFD group were infused with 90 mg/kg STZ and then fed with a high-fat diet or high-cholesterol and high-fat diet for 9 months, respectively; HFD + STZ group and HCFD + STZ group were fed with a high-fat diet or high-cholesterol and high-fat diet, respectively, for nine months (after 3 months, pigs were injected with 90 mg/kg STZ intravenously).

Results

The results showed the serum glucose concentrations were within the normal range in all groups except for HFD + STZ group and HCFD + STZ group. Animals fed with a high-fat diet for 9 months, did not develop apparent atherosclerotic lesions; nevertheless, atherosclerotic lesions were seen in animals fed with high-cholesterol and high-fat diets. Moreover, hyperglycemia accelerated atherosclerosis (lesions on the intimal surface of the abdominal aorta, 0.44 ± 0.29 vs. 0.28 ± 0.26) in minipigs.

Conclusions

High-fat/high-cholesterol and high-fat diet combined with low-dose streptozotocin successfully established T2DM in minipigs. High-fat diet could not induce apparent atherosclerosis lesions but high-cholesterol and high-fat diet could during the nine months period. Hyperglycemia accelerated atherosclerosis in the minipigs.

Background

Diabetes is one of the fastest-growing health challenges of the 21st century. The number of adults living with diabetes has triplicated over the past 20 years. According to the latest edition of the IDF Diabetes, 463 million adults are currently living with diabetes [1]. Diabetes mellitus is classified into T2DM characterized by a progressive reduction of insulin effect (insulin resistance) and accompanied by β cell reduction or secretion decline (β cell disorder), and T2DM, which accounts for about 90% of diabetes

patients worldwide [2]. Therefore, it is urgent to explore the pathogenesis of T2DM and develop strategies for disease prevention and treatment.

Glucose metabolism, including gene regulation and overall blood glucose homeostasis, has often been investigated in the T2DM animal model, most of which have been performed in rodents [3]. However, the exact molecular and biochemical mechanisms of the occurrence and development of human T2DM remain unclear, and the clinical treatment methods for T2DM are not satisfactory. Moreover, an effective drug developed based on rodent models has a low clinical translation efficacy [4].

In recent years, pigs have been increasingly used for human biomedical research as unique research tools for surgical procedural training. They share similar anatomy, physiology, size, key metabolizing enzymes, and genetics with humans. They have a high reproduction rate and are widely applied in food physiology, obesity, metabolism, and cardiovascular disease translation researchers. In developing new therapeutic measures, pigs have served as a bridge between classic rodent models and humans [5, 6]. The application of pigs in drugs (e.g., statins) and equipment testing (e.g., vascular stents) is considered to have high predictive value for subsequent translation to applications in human beings [7].

Pigs do not easily develop T2DM. According to Gerstein and Waltman [8], pigs may effectively accumulate and store energy in summer and then use it in winter. Such anabolic-lipogenic capacity is amplified when they become livestock, resulting in a large population of islet β cells in pigs. As a result, they become resistant to environmental factors causing diabetes (high-energy diet and less exercise). It takes a long time to induce diabetes in pigs through a high-fat diet. In addition, significant hyperglycemia symptoms cannot be obtained in pigs [9, 10].

In addition to hereditary models, non-hereditary rat models are also widely used in diabetes research. A high-fat diet combined with STZ is a very useful approach to induce T2DM in rats [11] due to its low cost and wide application range. In this study, we established and validated a T2DM model in pigs, which was then used to analyze the pathogenesis of diabetes.

Materials And Methods

Animals and treatments

A total of 24 male Bama minipigs, aged 5–6 months, weighing 12.6–15.2 kg, were purchased from Beijing Strong Century Minipigs Breeding Base. All the animals were housed in an environment with a temperature of 20–26 °C, a relative humidity of 40–70%, and a light/dark cycle of 12/12 hr. Animals were fed in a separate cage. All animal studies (including the euthanasia procedure) were done in compliance with the regulations and guidelines of PLA General Hospital institutional animal care and conducted according to the AAALAC and the IACUC guidelines (ID: 2018-D14-26).

Minipigs were randomly divided into five groups: control group, STZ + high fat group (STZ + HFD), STZ + high cholesterol and high fat group (STZ + HCFD), high fat + STZ group (HFD + STZ), and high cholesterol

and high fat + STZ group (HCFD + STZ) (Table 1). The animals in the control group were fed with conventional feed for nine months. Animals in STZ + HFD group and STZ + HCFD group were fed with a high-fat diet or high-cholesterol and high-fat diet, respectively, for nine months (Table 2) after intravenous injection of 90 mg/kg STZ (Sigma, s0130-5, prepared in 10% liquid with a citric acid-sodium citrate buffer solution at pH 4.2–4.5). Animals in HFD + STZ group and HCFD + STZ group were fed with a high-fat diet or high-cholesterol and high-fat diet, respectively, for nine months; after 3 months, pigs were injected with 90 mg/kg STZ intravenously. Feed was given at 3% of body weight and adjusted according to monthly changes in body weight.

Table 1
Grouping and Treatment of Laboratory Animals

Group	Number of animals (number)	Treatment
Control	4	Conventional feed for nine months
STZ + HFD	5	Fed with a high-fat diet for nine months after intravenous injection of 90 mg/kg STZ
STZ + HCFD	5	Fed with high cholesterol and high-fat diet for nine months after intravenous injection of 90 mg/kg STZ
HFD + STZ	5	Fed with a high-fat diet for three months → intravenous injection of 90 mg/kg STZ → fed with a high-fat diet for an additional six months
HCFD + STZ	5	Fed with high cholesterol and high-fat diet for three months → intravenous injection of 90 mg/kg STZ → fed with high cholesterol and high-fat diet for an additional six months

Table 2
The proportion of Main Components in Experimental Feed

Item	Unit	Control feed	High-fat feed	High cholesterol and high-fat feed
Weight proportion	Tallow (%)	0	15	15
	Cholesterol (%)	0	0	2
	Bile salt (%)	0	0.5	0.5
	Basic feed (%) *	100	84.5	82.5
Energy proportion	Fat (Kcal%)	10.66	43.57	46.58
	Protein (Kcal%)	23.39	17.68	17.14
	Carbohydrate (Kcal%)	65.96	38.75	36.28

* Basic feed formula: corn 64.15%, soybean meal 19%, bran 13%, stone powder 0.9%, calcium hydrogen phosphate 1.5%, salt 0.4%, additive 1%, tryptophan 0.05%.

Body weight and BMI

The body weight was measured once a month (8:30 – 10:30 a.m., fasting weight). Body length was measured on day 1 and after 3 and 9 months. Animals were restrained with slings, and the distance from the connecting line between the two ears to the tail root was measured. BMI was estimated according to the calculation method of the human clinical body mass index: $BMI = Weight (kg)/Length (m)^2$.

Fasting blood glucose (GLU), fasting serum insulin (INS), blood lipid indexes, and liver and kidney function indexes

Fasting blood glucose (GLU), fasting serum insulin (INS), blood lipid indexes (TG, TC, HDL-C, LDL-C, FFA), liver and kidney function indexes (ALT, AST, CRE, and BUN) were measured once a month (fasting blood glucose was determined by rapid blood glucose meter (Johnson & Johnson: ULtra). Insulin was detected by radioimmunoassay, XH6080 radioimmunoassay of Xi'an Instrument Factory. Other indexes were detected by Toshiba 120 automatic biochemical meter. Beijing Beijian Xinchuangyuan Biotechnology Co., Ltd. provided all the reagents, and the detection was completed by Beijing North Institute of Biotechnology Co., Ltd.).

Intravenous glucose tolerance (IVGTT) and insulin release test

Intravenous glucose tolerance (IVGTT) and insulin release test were performed once every three months. Briefly, animals were given 50% glucose injection (1.2 mL/kg) by intravenous injection from 8:00 a.m. to 11:00 a.m. after a night of fasting (15–18 h). The blood glucose was measured by a glucometer (Johnson & Johnson: Ultra) before (0 min) and 10, 30, 60, 90, and 120 minutes after the injection. At the same time point, 2 ml of blood was collected from the lateral saphenous vein of the forelimb, and the serum was taken to detect the insulin value (detection method: radioimmunoassay, reagent; detection were provided by Beijing North Institute of Biotechnology Research Institute Co., Ltd.)

Urine routine test and urine protein

Urine routine test and the urine protein were measured before and after treatment (after 9 months). Urine routine test: dry tablet method, Shenzhen Mejer Mejer-600 urine automatic analyzer and reagent were provided by Shenzhen Mejer; urine protein: biuret method and reagent were provided by Beijing Beijian Xinchuangyuan Biotechnology Co., Ltd.

Coronary CT

The Coronary CT scan was conducted after treatment (after 9 months). Anesthesia, induced by intramuscular injection of 25 mg/kg of Xylazine hydrochloride injection and 0.25 mg/kg of midazolam, was maintained by intravenous injection of 6 mg/kg of sodium pentobarbital. Consequently, the left lateral position was taken, and the coronary arteries of the heart were detected by Siemens SOMATOM

Definition Flash Shuangyuan CT. The test-Bolus technique was adopted to estimate the contrast agent dosage. A 15 ml of nonionic contrast agent (350 mgI/ml iodophor) was injected through the auricular vein with a flow rate of 3.0 ml/s using a double-barrel high-pressure syringe. A layer was selected at the level of the aortic root. The time-density curve was measured by automatic software to determine the scanning delay time, and then, coronary artery scanning was performed. The scanning range was performed from 1 cm below the carina of the trachea to 2 cm below the diaphragm. In addition, 50–60 ml of contrast agent was injected at a flow rate of 3 ml/s, followed by 30 ml of normal saline at the same flow rate. The scanning layer thickness was 0.6 mm, the rotating speed of the machine was 0.28 s/360°, the tube voltage was 120 kV, and the tube current was 222 mA. A prospective ECG gated scanning mode was adopted. The acquisition time window was 48%-72% of the cardiac cycle, and the scanning time was about 8 s.

Pathological examination

The pathological examination was conducted after treatment (after 9 months). After anesthesia (described above), the animals were bled to death through the femoral artery. Anatomy was carried out for examination and material acquisition.

Pancreas

The complete pancreas was carefully removed, weighed, and fixed in 4% formaldehyde solution. During the re-examination, two pieces of spleen lobe, two pieces of the duodenal lobe, and two pieces of connecting lobe at the center, 1 cm apart, were taken, and paraffin sections were routinely performed. Finally, samples were stained with HE staining and insulin immunohistochemical staining.

The proportion of islets in the pancreas was observed and calculated with HE staining sections, and two sections were calculated for each leaf (Image-Pro Plus 4.5 software). The proportion of positive cells in pancreatic tissue was observed and calculated by insulin staining sections, and two sections were calculated for each leaf (Image-Pro Plus 4.5 software). The proportion of islets in the pancreas and the proportion of insulin-positive cells (β cells) in the pancreas of each animal were calculated according to the average value obtained from six sections. The weight of islet cells was estimated by using the proportion of β cells in the pancreas and the weight of the pancreas; the relative weight of body weight was also calculated.

Abdominal aorta

The abdominal aorta was dissected and cut longitudinally, immersed in an oil red O solution for 6 min (saturated oil red O staining solution), and fixed in 4% neutral formaldehyde solution. During re-examination, the most obvious plaque bulge was taken, and paraffin sections were made. Finally, samples were stained with HE and observed under an optical microscope.

Measuring the proportion of atherosclerotic plaque in the intima of the abdominal aorta: the abdominal aorta between the renal artery branch at the cephalic end and the iliac artery branch at the caudal end

were selected, the range of diseased plaque was carefully marked, and the proportion of diseased plaque area to abdominal aorta area was calculated by Image-Pro Plus 4.5 software.

Coronary artery

At a distance of 0.5 cm from the heart's coronal adipose, the anterior descending branch of the left coronary artery was taken together with the myocardium and fixed with 4% neutral formaldehyde solution. Paraffin sections were made. Samples were then stained with HE and observed under the optical microscope.

Retina, liver, and kidney

Retina, liver, and kidney were dissected and fixed in 4% neutral formaldehyde solution. Paraffin sections were made. Samples were then stained with HE and observed under the optical microscope.

Ultrastructural pathology examination

Retina

The retina was dissected from the right side, 2 mm apart from the optic nerve tract, 0.5 × 0.5 cm of the whole layer of the eyeball wall, fixed with 2% phosphate-buffered glutaraldehyde at pH 7.2, and stored at 4°C. During re-examination, 5–6 pieces of 1 mm³ retinal tissues were re-fixed by 1% phosphate-buffered osmium tetroxide. Ultra-thin sections (dehydrated by acetone step by step and embedded in resin) were made, stained with uranium and lead, and observed by transmission electron microscope (HT7800 Hitachi 120kV transmission electron microscope).

Measurement of the capillary basement membrane was performed according to Siperstein *et al* [12]. Briefly, the area with obviously visible basement membrane and endothelial cell/adventitia cell boundary was selected for photographing for measurement of the capillary basement membrane (magnification × 5000 for retina; magnification × 3000 for kidney). A total of five blood vessels were selected for each animal, and 20 radiation lines were drawn from the center of the blood vessel lumen, after which the basement membrane thickness at the intersection of the radiation lines and the basement membrane was measured. Each blood vessel can obtain 10–15 effective basement membrane thickness values. Each animal's capillary basement membrane thickness was calculated according to the average of 50–75 measured values obtained.

Renal cortex

5–6 pieces of 1 mm³ renal tissue were dissected from the contralateral side of renal hilum 1 mm away from the capsule. Tissue fixation, ultrathin section making and staining and examination were the same as those of retina.

Statistical analysis

All data are presented as mean \pm standard error of the mean (SEM). Differences between experimental groups were analyzed using a one-way analysis of variance followed by post-hoc testing with an unpaired Student's t-test. Analyses were performed with GraphPad Software (GraphPad Software Inc., San Diego, CA, U.S.A.). P-values < 0.05 (two-tailed) were considered statistically significant.

Results

General observation

All animals in the control group were in good health. Animals in the STZ + HFD group and STZ + HCFD group had a smoother coat compared to the control group, and their weight gradually increased over time. Similar characteristics were observed in pigs in the HFD + STZ group and HCFD + STZ group during the first three months; yet, after the administration of STZ, the animals became listless and lost appetite. Three days after the administration of STZ, the animals recovered but then began to gradually lose weight. One animal in HCFD + STZ group showed signs of acidosis five months after the STZ administration, after which insulin therapy was given (insulin dose: 0.44 U/kg, subcutaneous injection, once a day (Levemir[®] Insulin Detemir Injection)). Moreover, one animal in the STZ + HCFD group developed a hind limb injury operation, which affected its eating; the data of this animal were not included in the statistical analysis. In addition, one animal in the HFD + STZ group and one in the HCFD + STZ group that did not develop hyperglycemia after administration of STZ were excluded from the final analysis.

Weight and BMI

Weight

The animals in the control group gradually increased their weight over time. The body weight of animals pre-treated with STZ (STZ + HFD group and STZ + HCFD group) increased faster than that of the control group, and the difference was significant ($P < 0.05$). Moreover, the body weight of HFD + STZ group and HCFD + STZ group increased faster than that of the control group ($P < 0.01$) in the first three months (before STZ administration); however, after the administration of STZ, the body weight decreased; yet no significant difference was found compared to the control group (Fig. 1).

BMI

Before the experiment, no difference in BMI values was observed between groups. During the first 3 months, the BMI of pigs fed with high-fat or high-cholesterol and high-fat diets gradually increased. Yet, due to large individual differences, no statistical differences were observed.

Nine months after the experiment, the BMI of all hyperglycemic animals (HFD + STZ group and HCFD + STZ group) further decreased compared to the 3-month time point; however, no statistical difference was obtained due to large individual differences (Fig. 1).

Fasting Blood Glucose (GLU), Fasting Serum Insulin (INS), and HOMA-IR Index

Fasting blood glucose (GLU)

During the experiment, the control group GLU value ranged between 3.2–4.2 mmol/L. The GLU level of animals pre-treated with STZ (STZ + HFD group and STZ + HCFD group) did not change much during the experiment; however, their values were higher than that of the control group during the first month (STZ + HFD group, $P < 0.05$) and the second month (STZ + HFD group and STZ + HCFD group; $P < 0.01$). The GLU levels of one animal in the HFD + STZ group and one in the HCFD + STZ group showed little change during the experiment (ranging between 2.9–4.9 mmol/L and 3.4–7.8 mmol/L, respectively), while the GLU levels of the other animals in those group significantly increased after STZ administration (ranging between 15.4–31.1 mmol/L and 10.3–29.4 mmol/L, respectively; $P < 0.01$) (Fig. 2A).

Fasting serum insulin (INS)

During the experiment, the control group INS value ranged from 8.36 to 17.64 μ IU/ml. The INS values of animals pre-treated with STZ (STZ + HFD group and STZ + HCFD group) were similar to the control group. The fasting insulin values of animals in the HFD + STZ group and HCFD + STZ group were not significantly different from those in the control group during the first three months; yet, after the administration of STZ, the INS gradually decreased (4th month, HCFD + STZ group, $P < 0.05$; 8th and 9th month, HFD + STZ group and HCFD + STZ group, $P < 0.05$) (Fig. 2B).

HOMA-IR

During the experiment, the control group HOMA-IR value ranged from 1.56 to 2.67. The HOMA-IR values of animals pre-treated with STZ (STZ + HFD group and STZ + HCFD group) were not significantly different from those of the control group. The HOMA-IR values of the FD + STZ group and HCFD + STZ group were not significantly different from that of the control group during the first three months, but then gradually increased after the administration of STZ ($P < 0.05$ or $P < 0.01$) (Fig. 2C).

IVGTT and insulin release test

IVGTT

Before the experiment, the fasting blood glucose level of the control group was 3.2–3.7 mmol/L, reaching the peak value of 12.3–14.7 mmol/L 10min after intravenous glucose administration and returning to the pre-glucose level of 3.1–4.8 mmol/L 60 min after intravenous glucose administration. There was no significant difference between the other groups and the control group (Fig. 3).

At the third month of the experiment, the peak value of all the experiment groups' blood glucose was slightly higher, and the recovery speed of blood glucose was slower than that of the control group. At 30min, the peak value of blood glucose in the STZ + HFD group ($P < 0.01$), STZ + HCFD group ($P < 0.05$),

and HCFD + STZ group ($P < 0.05$) was higher than that of the control group. At 60 min, the peak value of blood glucose was higher in STZ + HFD group ($P < 0.01$), HFD + STZ group ($P < 0.05$), and HCFD + STZ group ($P < 0.05$) than in the control group. At 90 min, the peak value of blood glucose was higher in the STZ + HFD group and HFD + STZ group than in the control group ($P < 0.05$). At 120 min, the peak value of blood glucose was higher in the STZ + HFD group than in the control group ($P < 0.05$).

The IVGTT curves of animals pre-treated with STZ (STZ + HFD group and STZ + HCFD group) showed no difference with the control group at the sixth and ninth months. At six months after the experiment, the IVGTT curves in the HFD + STZ group and HCFD + STZ group were all above the glucose tolerance curves of the control group, i.e., the blood glucose values at all time points were significantly higher than those of the control group ($P < 0.01$), the blood glucose values recovered slowly, and were still significantly higher than those before glucose administration 60 min and 90 min after glucose injection ($P < 0.01$). However, there was no significant difference between HFD + STZ group and HCFD + STZ group ($P > 0.05$). The IVGTT curve of the group that was given STZ later at the ninth month was similar to that in the sixth month.

Insulin release test

Before the experiment, the control group fasting serum insulin value was 7.52–13.92 $\mu\text{IU/ml}$, reaching the peak value of 25.84–62.62 $\mu\text{IU/ml}$ 10–30 min after intravenous glucose administration, and returning to the pre-glucose level of 6.42–21.17 $\mu\text{IU/ml}$ at 60 min. There was no significant difference between the other groups and the control group (Fig. 4).

The changes in serum insulin values of groups pre-treated with STZ (STZ + HFD group and STZ + HCFD group) were not significantly different from those of the control group at the 3rd, 6th, and 9th month but were all higher than those of the control group at certain time points (STZ + HCFD group, the sixth month, 30min after glucose injection, $P < 0.01$). The changes in serum insulin values in HFD + STZ group and HCFD + STZ group after intravenous glucose injection were not significantly different from those in the control group on day one and after three months; yet, after the administration of STZ, the secretion of insulin significantly decreased. At six months and nine months, the serum insulin after intravenous glucose injection did not significantly increase, and the insulin secretion regulation ability regulated by blood sugar was lost.

Changes of Biochemical Blood Indexes during the Experiment

TG

The average value of serum TG in the control group changed from 0.29 mmol/L to 0.83 mmol/L during the experiment. There was no significant difference between the STZ + HFD group and HFD + STZ group, and the control group during the experiment. In addition, no significant difference was observed between HFD + STZ group and HCFD + STZ group, and the control group at three months. After STZ

administration, the serum TG concentration was higher than that of the control group for most of the time (HFD + STZ group, the fourth, eighth, and ninth months, $P < 0.01$ or $P < 0.05$; HCFD + STZ group, the sixth and seventh months, $P < 0.05$) (Fig. 5A).

TC

During the experiment, the average value of serum TC in the control group ranged from 1.87 mmol/L to 2.59 mmol/L. There was no significant difference between all animals fed with high-fat diet (STZ + HFD group and HFD + STZ group) and the control group. The serum TC values of all animals fed with high cholesterol and a high-fat diet (STZ + HCFD group and HCFD + STZ group) were significantly higher than those of the control group ($P < 0.01$), with an average value of 8.44–14.22 mmol/L, which was 4.5–5.5 times higher than that of the control group (Fig. 5B).

HDL-C

During the experiment, the average value of serum HDL-C in the control group ranged from 0.6 to 0.99 mmol/L. The serum HDL-C values of all animals fed with high cholesterol and high-fat diet (STZ + HCFD group and HCFD + STZ group) were significantly higher than those of the control group ($P < 0.01$), with an average value of 1.91–3.41 mmol/L (3.2–3.4 times higher than that of the control group). The serum HDL-C value of STZ + HFD group was also significantly higher than that of the control group ($P < 0.01$; 2.6–2.7 times higher than that of the control group). The serum HDL-C value of HFD + STZ group was higher than that of the control group in the first three months ($P < 0.01$). There was no significant difference between HFD + STZ group and the control group after five months (Fig. 5C).

LDL-C

During the experiment, the average value of serum LDL-C in the control group fluctuated from 0.77 mmol/L to 1.52 mmol/L. There was no significant difference between all animals pre-treated with STZ (STZ + HFD group and HFD + STZ group) and the control group. The serum LDL-C values of all animals fed with high cholesterol and high-fat diet (STZ + HCFD group and HCFD + STZ group) were significantly higher than those of the control group ($P < 0.01$), with an average value of 3.96–11.05 mmol/L, which was 5.1–7.3 times higher compared to the control group.

FFA

The average value of serum FFA in the control group ranged from 0.14 mmol/L to 0.67 mmol/L during the experiment. The serum FFA values of groups given STZ first (STZ + HFD group and HFD + STZ group) were not significantly different from those of the control group during the experiment. The serum FFA values of groups post-treated with STZ (HFD + STZ group and HCFD + STZ group) were significantly higher than those of the control group at most time points after STZ administration (HFD + STZ group, from the third to the ninth months, $P < 0.05$; HCFD + STZ group, the fourth and the eighth month, $P < 0.05$).

ALT, AST, ALB, GGT, CRE, and BUN

During the experiment, these indexes of serum liver function and renal function of all animals fluctuated within the normal range, and the measured values of each group of animals did not change much; no difference was found compared with the control group. The average value of fasting serum HbA1c in the control group fluctuated between 3.2% and 4.7%, while the average value of HbA1c in other groups fluctuated between 2.9% and 4.7%.

Urine routine test and urinary protein

Urine routine test

During the experiment, no abnormality was found in the urine routine examination of the animals in the control group, while urine white blood cells, red blood cells, and protein were all negative. The urine routine test of STZ + HFD group and STZ + HCFD group did not significantly differ from that of the control group. The urine GLU of HFD + STZ group and HCFD + STZ group were both +++.

Urine protein

During the experiment, urine routine examination protein was negative. Yet, a small amount of protein was detected by using more sensitive detection methods. There was no significant difference in urine trace protein between each group and the control group (Fig. 6).

Islets/pancreas and β cells/body weight

The shape and size of the pancreas of the control pigs were normal, showing three leaves, namely spleen, duodenum, and connecting leaf. The weight ratio of the pancreas to body weight was 0.09%-0.15%, with large individual variation (SD = 0.023). No difference in pancreas mass was observed between the experimental groups and the control group (Figs. 7, 8).

Under the optical microscope, the control group islets were scattered, showing different and generally small size. Most cell cluster-like ultra-small islets were composed of several or more endocrine cells. Under HE staining conditions, control group islet cells were relatively lightly stained and were clearly distinguished from exocrine glands. The boundaries of islets were regular. Insulin immunohistochemical staining showed that positive insulin cells (β cells) accounted for the vast majority of cells.

In order to examine whether STZ can cause injury to islets and the severity of the injury, we calculated the proportion of islets to the pancreas and the proportion of islet β cells to body weight of animals in each group. The results showed that in the control group, the proportion of islets in the pancreas was 1.52%-4.98% ($3.15 \pm 1.42\%$), and the proportion of β cells in body weight was 0.012‰-0.024‰ ($0.020 \pm 0.006\%$). Compared with the control group, the proportion of islets in the pancreas and the proportion of β cells in body weight of animals given STZ first significantly decreased ($P < 0.01$), with an average decrease of 64.7% (STZ + HFD group) and 71.4% (STZ + HCFD group). These values were even lower in animals who received STZ after three months (the average reduction of islet β cells was 87.3% (HFD + STZ group) and 83.1% (HCFD + STZ group), respectively); a significant difference was observed compared to the control groups, STZ + HFD group, and STZ + HCFD group ($P < 0.05$). There was no

significant difference between the two groups of animals given STZ first, and between the two groups of animals given STZ later.

Morphologically, the above counting results were further supported. Compared with the control group, the number of islets in animals pre-treated with STZ was significantly reduced, and the boundary between islets and exocrine glands was irregular; however, HE stained islet cells were lightly stained and clearly distinguished from exocrine glands. Insulin immunohistochemical staining indicated that the proportion of β cells in islets was also significantly reduced. It is speculated that after STZ administration, a large number of islet β cells died and were absorbed, resulting in islet shrinkage and collapse. The results of islet deformation caused by exocrine gland extrusion have not been fully recovered.

There was no significant difference between the STZ + HFD group and the STZ + HCFD group. The number of islets of the animals that received STZ after 3 months was more obviously decreased; the boundary between islets and exocrine glands was irregular, and the proportion of β cells in islets were more prominently decreased. In addition, a large number of deeply stained cells appeared in many islets under HE staining conditions, making it difficult to distinguish islets from exocrine glands. Cell regeneration is obvious in the islets of the pancreas. There was no significant difference between HFD + STZ group and HCFD + STZ group.

Under an optical microscope, there was no obvious abnormality in the retina of animals in each group. After observing the retina under the transmission electron microscope, the complete capillary position in the section was selected, and the thickness of the retinal capillary basement membrane was measured. The thickness of the basement membrane of retinal capillaries in the control group was 94.8 ± 2.2 nm. Compared with the control group, the thickness of basement membrane of retinal capillaries in the HFD + STZ group and HCFD + STZ group showing hyperglycemia during a period of six months increased significantly and were 130.8 ± 5.5 nm ($P < 0.01$) and 134.8 ± 6.3 nm ($P < 0.01$), respectively (Fig. 9).

Kidney

Under an optical microscope, no obvious abnormality was found in the kidney structure of each group of animals. Yet, after using the transmission electron microscope, the thickness of the glomerular capillary basement membrane was measured. The basement membrane thickness of glomerular capillaries in the control group was 200.9 ± 2.6 nm. Compared with the control group, the basement membrane thickness of glomerular capillaries in the HFD + STZ group and HCFD + STZ group showing hyperglycemia during a period of six months were 275.7 ± 24.5 nm ($P < 0.05$) and 297.3 ± 16.5 nm ($P < 0.01$), respectively (Fig. 10).

Coronary artery

Coronary CT examination showed that the intima of coronary artery in all animals was smooth, and no obvious lumen stenosis, intimal thickening, or plaque lesion was found. Histopathological examination of the base of the anterior descending branch of the left coronary artery revealed that two animals in STZ + HCFD group had a mild fatty streak, and three animals in HCFD + STZ group had mild fatty streak (Fig. 11).

Abdominal aorta

There were no abnormalities in the control group. The intimal lesions of the abdominal aorta in animals fed with a high-fat diet (STZ + HFD group and HFD + STZ group) were slight, with a slight fatty streak, mainly distributed in the branches of arteries. The abdominal aortic intimal lesions of animals fed with high cholesterol and high-fat diet (STZ + HCFD group and HCFD + STZ group) were obvious with plaque lesions of different degrees. In the STZ + HCFD group, two animals showed slight fatty streak, and two showed obvious plaque lesions; one animal had serious lesions, and the plaque area accounted for 64.6% of the intima. In the HCFD + STZ group, plaque lesions were found in the intima of the abdominal aorta in all animals, and the proportion of plaque lesions in the intima of the abdominal aorta in two animals was > 50% (50.3% and 80.3%, respectively). Histopathological examination showed that the plaque lesion of the abdominal aorta intima was a stable fibrous plaque with a thick fibrous layer. Mild secondary lesions, mainly mineralization and cholesterol deposition, could be found in the deep layer of the plaque (Fig. 12).

Discussion

T2DM model

A high-energy diet can be used to induce type 2 diabetes in animals. So far, many diabetic animal models have been established.

In 2000, Reed *et al* [13] proposed a method for inducing insulin resistance in rats by using a high-fat diet and a low-dose streptozotocin (STZ). Later, Srinivasan *et al* [11] further modified and improved this model by testing four STZ doses (25, 35, 45, and 55 mg/kg) and using insulin secretion stimulating agent (glipizide) and insulin-sensitive agent (pioglitazone) to verify the insulin resistance and insulin secretion. They suggested a high-fat feeding for two weeks and 35 mg/kg STZ to induce a type 2 diabetes model in rats. Consequently, this approach has become the most commonly used T2DM model worldwide. This method can induce diabetic phenotype symptoms in a relatively short test period. Yet, when using pigs, this approach may not be enough [10, 14].

Some research suggested that a similar effect could be achieved in pigs by feeding animals with high-fat feeding for three months as two weeks feeding in rats [10, 15]. To achieve significant hyperglycemia, in this study, 90 mg/kg STZ was used. This dosage was selected based on previous rat model studies [11, 13] and our previous research results in minipigs.

In this experiment, Bama minipigs were fed with high-fat/high-cholesterol high-fat diet for three months. The body weight of animals without STZ was significantly higher than that of the control group. Although the fasting blood glucose and fasting insulin values were not significantly different from the control group, in the IVGTT experiment, the area under the blood glucose curve after glucose administration was larger than that of the control group (the blood glucose values at multiple time points after glucose

administration was significantly higher than that of the control group, and the recovery of blood glucose values was slowed). The blood lipid levels (TC, HDL-C, and LDL-C) were also increased. These results were consistent with that of Larson *et al* [15]. All of this suggested a mild insulin resistance.

In animals treated with 90 mg/kg STZ, fasting blood glucose increased compared to the control group. During hyperglycemia, the glucose tolerance of animals was impaired, but insulin secretion capacity still existed. IVGTT test showed that the insulin secretion level did not significantly increase after glucose administration, showing insufficient insulin secretion. This indicated that the Bama minipig T2DM model with significant hyperglycemia symptoms could be successfully established by feeding a high-fat or high-cholesterol and high-fat diet for three months and then applying 90 mg/kg STZ. The hyperglycemia symptoms can last for at least six months.

Recently, Yanjun *et al* [16] successfully established a type 2 diabetes model in Bama minipigs by using a similar method. They fed pigs with a high-sucrose and high-fat diet for six months, followed by an IV injection of 60 mg/kg STZ. Hyperglycemia symptoms continued until the end of the experiment (four months). These data suggested that a model can be established using a lower concentration of STZ; yet, it takes a longer time to establish a model.

Toxic effect of STZ on islet β cells

STZ has a selective toxic effect on islet β cells and relatively low toxicity to other tissue. The chemical composition of STZ is methyl-1-nitrosyl-C2-D glucose. Once STZ enters the body, it binds a GLUT2 receptor expressed on the β cells, causing DNA strand breakage, after which, repair mechanism is activated, which reduces nicotine adenine diglycoside nucleic acid and ATP, and in turn, leads to cell death[17].

The effect of STZ is related to the expression of glucose transporter GLUT2. The difference in toxicity to STZ between different animal species may result from different expression levels of GLUT2 [18–20]. Dufrane *et al* [18] showed that compared with rats and macaques, pigs express less GLUT2 receptors. Therefore, in pigs, a large dose of STZ is required to destroy a sufficient number of islet β cells, thus causing diabetes. Dufrane *et al* also suggested that 150 mg/kg STZ could be used to destroy 97% of islet β cells in Landrace pigs, resulting in persistent diabetes. This result is consistent with our previous research results using Bama minipigs.

In this study, we used 90 mg/kg STZ and found that the application of STZ before or after high-fat/high-cholesterol and high-fat diet feeding may lead to different effects. The pre-application of STZ caused substantial damage to islet β cells, which was further confirmed by pathological examination (the number of islet β cells in minipigs with pre-application of STZ was significantly lower than that in the control group, and the morphological structure of islets could not completely recover to normal at nine months after STZ injection). However, nine months after treatment, the concentrations of fasting blood glucose and insulin were not significantly different in animals with pre-application of STZ and control pigs. In contrast, after three months of high-fat/high-cholesterol and high-fat feeding and the same dose

of STZ, the animals showed significant hyperglycemia. The reason for such a difference in sensitivity to STZ toxicity is presumed to be related to the expression level of GLUT2 in islet β cells.

Minipigs have a large number of islet β cell reserves [8]. Under normal feeding conditions, only a part of islet β cells are active, and the secreted insulin is sufficient to meet the needs of body blood glucose regulation. When feeding animals with a high-fat diet, they need more insulin to metabolize excess energy intake. Therefore, more islet β cells are activated, which then increases insulin secretion. The active islet β cells express more GLUT2 on the surface to transport more glucose. However, higher expression of GLUT2 receptor leads to higher STZ uptake. Therefore, STZ doses of 60 mg/kg in Yanjun's experiment [16] and 90 mg/kg in our study do not cause blood glucose changes in minipigs under normal feeding conditions, but can induce damage to a large number of islet β cell in minipigs fed with high-fat diet, thus causing animal insulin secretion to fail to meet the needs of body metabolism, and eventually turning into diabetes.

Changes in the number of islet β cells in T2DM

T2DM is characterized by insulin resistance and insufficient insulin secretion. However, it is unclear whether this insulin secretion is caused by a decrease in the number of islet β cells, a substantial defect in secretion capacity, or both. Studies have shown that most patients with T2DM, whether fat or thin, have an absolute decrease in the number of islet β cells [21, 22]. It is worth noting that these evaluations on the number of β cells are mainly based on autopsy studies, not prospective studies. Therefore, knowing the number of β cells before onset is of crucial importance. In this study, two experimental groups received 90 mg/kg STZ in advance (pre-treatment). According to previous research results, it is predicted that although this dose of STZ does not cause hyperglycemia, it tends to cause a significant reduction in the number of islet β cells. Pathological examination results further confirmed this prediction result. However, there was no significant difference in fasting blood glucose and fasting insulin concentration between these animals and the control group, whether they were fed with a high-fat diet or high-cholesterol and high-fat diet for nine months. The animals' weight was increasing, showing a trend toward obesity. There was no abnormality in any of the liver function and renal function with detected indexes, which shows that although the number of islet β cells was significantly reduced, the susceptibility of Bama minipigs to T2DM did not increase after nine months of treatment with high-fat or high-cholesterol high-fat feed [10]. Therefore, we speculate that, although there are individual differences in the number of islet β cells during growth and development, the absolute decrease in the number of islet β cells in patients with T2DM is the consequence of disease occurrence and development, which may be related to the difference in susceptibility of individual animal islet β cells to pathogenic factors, and is irrelevant to the number of pre-existing islet β cells.

The relationship between diabetes mellitus, high-fat diet, and atherosclerosis

Diabetic patients are 2–6 times more likely to develop atherosclerosis than non-diabetic patients [23]. Coronary heart disease is the most common fatal factor for adult diabetic patients [24]. Up to 80% of

patients with type 2 diabetes die of atherosclerotic macrovascular disease. Since wild-type mice and rats do not easily develop atherosclerosis, and experiments in transgenic mice have indicated that diabetes has a weak effect on promoting atherosclerosis [25], pigs spontaneously develop atherosclerosis with increasing age and in which diabetes can aggravate atherosclerosis are of utmost importance [26, 27].

In this study, obvious atherosclerotic plaque lesions in the abdominal aorta and iliac artery and mild fatty streak lesions of coronary arteries were observed in animals fed with high-cholesterol and high-fat diet (STZ + HCFD group and HCFD + STZ group), which is basically consistent with our previous research results [28]. The proportion of abdominal aortic plaque lesion to the intimal area was used as an indicator of the severity of atherosclerosis. The results showed that diabetes could aggravate atherosclerosis induced by high-cholesterol and a high-fat diet, which is consistent with Gerrity *et al* [26]. Unfortunately, the coronary artery lesions of minipigs in this experiment were mild. After 90 days of high-cholesterol and high-fat feeding and 60 days of diabetes, no obvious lesions were detected by the coronary CT. Pathological examination showed that only a few animals had mild fatty streak lesions in coronary arteries, which is inconsistent with the research results in other pig models [26, 27].

It is believed that saturated fatty acids (SFAs) in food increase the level of serum cholesterol, thus increasing the risk of atherosclerosis. Although Siri-tarino *et al* [29] admitted that replacing saturated fat with unsaturated fat is beneficial in preventing ischemic heart disease compared with carbohydrates, they proposed no clear evidence for the relationship between SFA intake and cardiovascular diseases [30]. Scholars investigating the effect of diet insist that SFA intake should be reduced to 6–7% of total calories in a diet with a balanced and reasonable nutritional structure [31]. Since these studies all come from statistical analysis of clinical data, they are inevitably affected by patients' heredity, disease background, and other conditions.

The study of animal models can selectively control the experimental conditions and provide a reliable tool for further analysis of SFA's mechanism. Our data suggested no difference in the occurrence and severity of atherosclerosis compared with the normal diet by simply increasing the content of saturated fatty acids in the feed of Bama minipig. Moreover, besides increased high-density lipoprotein cholesterol (HDL-C), serum triglyceride (TG), total cholesterol (TC), low-density lipoprotein cholesterol (LDL-C), and free fatty acid (FFA) did not increase, which is consistent with previous studies [32]. In addition, this study further confirmed that cholesterol has an important role in the occurrence and development of atherosclerosis. As a risk factor, cholesterol is significantly higher than diabetes.

About diabetic microangiopathy and complications

Diabetic microangiopathy is one of the most vital factors causing persistent complications; yet, its pathogenesis is not completely clear. In the present study, we observed the retina and kidney changes, which are the most common microvascular complications of diabetes mellitus.

Diabetic ophthalmopathy, which includes diabetic retinopathy (DR) and diabetic macular edema (DMO), is the most common microvascular complication of diabetes [33]. It is also the main cause of blindness

in working-age adults [33]. Before clinical symptoms appear, DR has undergone some histological changes. These early morphological changes include capillary basement membrane thickening, pericyte loss or ghost remnants, acellular capillary structure, endothelial cell proliferation, and microaneurysm formation. Capillary basement membrane thickening is considered the most common and consistent feature in the early stage of DR, which is commonly used as an early marker of experimental DR. In this study, four animals in each group treated with STZ later experienced significant hyperglycemia that lasted six months. No obvious abnormalities were found under conventional tissue sections, HE staining, and optical microscope of miniature pig retina. Consequently, the thickness of the capillary basement membrane was measured using a transmission electron microscope. It was found that the retinal capillary basement membrane of diabetic minipigs was significantly thickened, which was basically consistent with the research results of Lee *et al* [34] and Hainsworth *et al* [35]. Lee and colleagues induced type 1 diabetes in Yorkshire pigs with STZ (150 mg/kg). Five diabetic pigs were obtained in this experiment; retinal capillary basement membrane thickening was detected in three pigs, which first occurred at the 18th week of hyperglycemia, and was not detected in the other two pigs, with detection being carried out in the 18th and 26th weeks of diabetes respectively. Hainsworth *et al* induced type 1 diabetes of Yucatan miniature pigs with alloxan (150–200 mg/kg). After 20 weeks of diabetes, the retinal capillary basement membrane thickened (five). Interestingly, in their study, the diabetic pigs (six) fed with a high-fat diet were the same as the control group, and the capillary basement membrane did not thicken. In our study, diabetic animals were fed with a high-fat or high-cholesterol and high-fat diet. The detection time was 24 weeks after suffering from diabetes, and the retinal capillary basement membrane was definitely thickened.

Diabetic nephropathy is the main cause of end-stage renal disease worldwide, with 35% of diabetic patients progressing to severe chronic renal disease [36]. Histopathological findings of diabetic nephropathy include glomerular capillary basement membrane thickening, mesangial dilatation, mesangial sclerosis, and vascular lesions, such as hyaline degeneration [37]. In this study, diabetic minipigs experienced continuous and significant hyperglycemia for six months. Serum GRE and BUN showed no significant difference compared to the control group. Except for urine sugar index, there was no obvious abnormality in the urine routine test and micro-urine protein detection. In addition, the optical microscope examination showed that there was no obvious abnormality in renal tissue morphology. However, the glomerular capillary basement membrane thickened. These results are consistent with Khairoun *et al* [38] and Maile *et al* [39]. Maile and colleagues induced diabetes in Yorkshire pigs with STZ (150 mg/kg) for 22 weeks. They observed an increase in glomerular mesangial coefficient and thickening of the capillary basement membrane. Khairoun *et al* induced diabetes in pigs (Landrace x Yorkshire, T-line) with STZ (140 mg/kg) fed with an atherosclerotic diet for 15 months. They observed thickening of the glomerular capillary basement membrane (only typical individuals were detected), and glomerular mesangium showed a trend of expansion. At this time, no abnormality was found in clinical indexes (serum CRE level, urine albumin/creatinine ratio).

Clinically, ocular microvessels are often used as indicators of diabetic microangiopathy. This study showed that in the Bama minipig T2DM model, the symptoms of diabetes lasted for six months, and the

conventional clinical indicators of microvascular complications did not show abnormalities. However, the retina and kidney's capillary basement membrane was thickened, which could be used as an indicator for the pathogenesis research and treatment evaluation of early microvascular diseases.

Conclusions

A high-energy diet can be used to induce T2DM in many kinds of animals. But the long inducing duration restrains its usage. Nowadays, the rat T2DM induced by high-fat feeding combined with low dose STZ has becoming the most popular used model. We followed the same way to establish the T2DM model in minipigs. And the results showed that after fed with High-fat/high-cholesterol and high-fat diet for 3 months, the infusion of 90 mg/kg STZ can successfully establish a T2DM model with significantly high blood glucose level in Bama minipigs(incidence rate 80%). Also, we found that the high-fat diet alone could not induce accelerated atherosclerosis during the 9 month inducing period, and the diabetes could accelerate the high-cholesterol diet induced atherosclerosis in minipigs.

Declarations

Acknowledgments

This work was supported by the Specialized Research Fund for National Natural Science Foundation of China (No. 31472057 and 31900379) and Special Scientific Research Project of Army Laboratory Animals (No.SYDW[2017]03).

Authors' contributions

HC, GW, and YZ designed and performed experiments and analyzed data. MN, YJ, JY, LX, XD performed the experiments. All authors read and approved the final manuscript.

Funding

The study was supported by the National Natural Science Foundation of China (No. 31472057 and 31900379) and Special Scientific Research Project of Army Laboratory Animals(No.SYDW[2017]03).

Conflict of Interest

We certify that there is no conflict of interest with any financial organization regarding the material discussed in the manuscript.Chen Hua is the guarantor of this work, and, as such, had full access to all the data in the study and takes responsibility for the integrity of the data and the accuracy of the data analysis.

Ethics approval and consent to participate

All animal studies were done in compliance with the regulations and guidelines of PLA General Hospital institutional animal care and use committee. The treatment of animals in all experiments conforms to the ethical standards of experimental animals.

Author details

Yuqiong Zhao, Laboratory Animal Center, Chinese PLA General Hospital, Beijing, PR China; Email: zhaoyuqiong@163.com

Miaomiao Niu, Laboratory Animal Center, Chinese PLA General Hospital, Beijing, PR China; Email: paper222@126.com

Yunxiao Jia, Laboratory Animal Center, Chinese PLA General Hospital, Beijing, PR China; Email: jiayunxiao89@126.com

Jifang Yuan, Laboratory Animal Center, Chinese PLA General Hospital, Beijing, PR China; Email: Yuanjifang@163.com

Lei Xiang, Laboratory Animal Center, Chinese PLA General Hospital, Beijing, PR China; Email: 18611990857@163.com

Xin Dai, Laboratory Animal Center, Chinese PLA General Hospital, Beijing, PR China; Email: daixin258@sina.com

Hua Chen, Laboratory Animal Center, Chinese PLA General Hospital, Beijing, PR China; Email: chenhua301paper@163.com

Guisheng Wang, Radiology Department of No.3 Clinical Center, Chinese PLA General Hospital, Beijing, PR China; Email: wanggs1996@tom.com

References

1. Williams R, Karuranga S, Malanda B, et al. Global and regional estimates and projections of diabetes-related health expenditure: Results from the International Diabetes Federation Diabetes Atlas, 9th edition. *Diabetes Res Clin Pract* 2020; 162: 108072.
2. American Diabetes A. Diagnosis and classification of diabetes mellitus. *Diabetes Care*. 2012;35(Suppl 1):64–71.
3. Sasase T, Yokoi N, Pezzolesi MG, et al. Animal models of diabetes and metabolic disease 2014. *J Diabetes Res* 2015; 2015: 571809.
4. Ali Z, Chandrasekera PC, Pippin JJ. Animal research for type 2 diabetes mellitus, its limited translation for clinical benefit, and the way forward. *Altern Lab Anim*. 2018;46(1):13–22.

5. Bahr A, Wolf E. Domestic animal models for biomedical research. *Reprod Domest Anim.* 2012;47(Suppl 4):59–71.
6. Renner S, Dobenecker B, Blutke A, et al. Comparative aspects of rodent and nonrodent animal models for mechanistic and translational diabetes research. *Theriogenology.* 2016;86(1):406–21.
7. Hasler-Rapacz J, Kempen HJ, Princen HM, et al. Effects of simvastatin on plasma lipids and apolipoproteins in familial hypercholesterolemic swine. *Arterioscler Thromb Vasc Biol.* 1996;16(1):137–43.
8. Gerstein HC, Waltman L. Why don't pigs get diabetes? Explanations for variations in diabetes susceptibility in human populations living in a diabetogenic environment. *CMAJ.* 2006;174(1):25–6.
9. Bellinger DA, Merricks EP, Nichols TC. Swine models of type 2 diabetes mellitus: insulin resistance, glucose tolerance, and cardiovascular complications. *ILAR J.* 2006;47(3):243–58.
10. Chen H, Liu YQ, Li CH, et al. The susceptibility of three strains of Chinese minipigs to diet-induced type 2 diabetes mellitus. *Lab Anim (NY).* 2009;38(11):355–63.
11. Srinivasan K, Viswanad B, Asrat L, et al. Combination of high-fat diet-fed and low-dose streptozotocin-treated rat: a model for type 2 diabetes and pharmacological screening. *Pharmacol Res.* 2005;52(4):313–20.
12. Siperstein MD, Unger RH, Madison LL. Studies of muscle capillary basement membranes in normal subjects, diabetic, and prediabetic patients. *J Clin Invest.* 1968;47(9):1973–99.
13. Reed MJ, Meszaros K, Entes LJ, et al. A new rat model of type 2 diabetes: the fat-fed, streptozotocin-treated rat. *Metabolism.* 2000;49(11):1390–4.
14. Torres-Rovira L, Astiz S, Caro A, et al. Diet-induced swine model with obesity/leptin resistance for the study of metabolic syndrome and type 2 diabetes. *ScientificWorldJournal* 2012; 2012: 510149.
15. Larsen MO, Rolin B, Wilken M, et al. High-fat high-energy feeding impairs fasting glucose and increases fasting insulin levels in the Gottingen minipig: results from a pilot study. *Ann N Y Acad Sci.* 2002;967:414–23.
16. Wu Y, Zhang L, Liang J, et al. Comparative analysis on liver transcriptome profiles of different methods to establish type 2 diabetes mellitus models in Guangxi Bama mini-pig. *Gene.* 2018;673:194–200.
17. Okamoto H. The role of poly(ADP-ribose) synthetase in the development of insulin-dependent diabetes and islet B-cell regeneration. *Biomed Biochim Acta.* 1985;44(1):15–20.
18. Dufrane D, van Steenberghe M, Guiot Y, et al. Streptozotocin-induced diabetes in large animals (pigs/primates): role of GLUT2 transporter and beta-cell plasticity. *Transplantation.* 2006;81(1):36–45.
19. Schnedl WJ, Ferber S, Johnson JH, et al. STZ transport and cytotoxicity. Specific enhancement in GLUT2-expressing cells. *Diabetes.* 1994;43(11):1326–33.
20. Elsner M, Tiedge M, Lenzen S. Mechanism underlying resistance of human pancreatic beta cells against toxicity of streptozotocin and alloxan. *Diabetologia.* 2003;46(12):1713–4.

21. Sakuraba H, Mizukami H, Yagihashi N, et al. Reduced beta-cell mass and expression of oxidative stress-related DNA damage in the islet of Japanese Type II diabetic patients. *Diabetologia*. 2002;45(1):85–96.
22. Butler AE, Janson J, Bonner-Weir S, et al. Beta-cell deficit and increased beta-cell apoptosis in humans with type 2 diabetes. *Diabetes*. 2003;52(1):102–10.
23. Kannel WB, McGee DL. Diabetes and cardiovascular disease. The Framingham study. *JAMA*. 1979;241(19):2035–8.
24. Haffner SM, Lehto S, Ronnema T, et al. Mortality from coronary heart disease in subjects with type 2 diabetes and in nondiabetic subjects with and without prior myocardial infarction. *N Engl J Med*. 1998;339(4):229–34.
25. Kako Y, Huang LS, Yang J, et al. Streptozotocin-induced diabetes in human apolipoprotein B transgenic mice. Effects on lipoproteins and atherosclerosis. *J Lipid Res*. 1999;40(12):2185–94.
26. Gerrity RG, Natarajan R, Nadler JL, et al. Diabetes-induced accelerated atherosclerosis in swine. *Diabetes*. 2001;50(7):1654–65.
27. Hamamdžić D, Wilensky RL. Porcine models of accelerated coronary atherosclerosis: role of diabetes mellitus and hypercholesterolemia. *J Diabetes Res* 2013; 2013: 761415.
28. Zhao Y, Xiang L, Liu Y, et al. Atherosclerosis Induced by a High-Cholesterol and High-Fat Diet in the Inbred Strain of the Wuzhishan Miniature Pig. *Anim Biotechnol*. 2018;29(2):110–8.
29. Siri-Tarino PW, Sun Q, Hu FB, et al. Saturated fatty acids and risk of coronary heart disease: modulation by replacement nutrients. *Curr Atheroscler Rep*. 2010;12(6):384–90.
30. Siri-Tarino PW, Sun Q, Hu FB, et al. Meta-analysis of prospective cohort studies evaluating the association of saturated fat with cardiovascular disease. *Am J Clin Nutr*. 2010;91(3):535–46.
31. Stamler J. Diet-heart: a problematic revisit. *Am J Clin Nutr*. 2010;91(3):497–9.
32. Hooper L, Martin N, Abdelhamid A, et al. Reduction in saturated fat intake for cardiovascular disease. *Cochrane Database Syst Rev* 2015; (6): CD011737.
33. Cheung N, Mitchell P, Wong TY. Diabetic retinopathy. *Lancet*. 2010;376(9735):124–36.
34. Lee SE, Ma W, Rattigan EM, et al. Ultrastructural features of retinal capillary basement membrane thickening in diabetic swine. *Ultrastruct Pathol*. 2010;34(1):35–41.
35. Hainsworth DP, Katz ML, Sanders DA, et al. Retinal capillary basement membrane thickening in a porcine model of diabetes mellitus. *Comp Med*. 2002;52(6):523–9.
36. Qi C, Mao X, Zhang Z, et al. Classification and Differential Diagnosis of Diabetic Nephropathy. *J Diabetes Res* 2017; 2017: 8637138.
37. Tervaert TW, Mooyaart AL, Amann K, et al. Pathologic classification of diabetic nephropathy. *J Am Soc Nephrol*. 2010;21(4):556–63.
38. Khairoun M, van den Heuvel M, van den Berg BM, et al. Early systemic microvascular damage in pigs with atherogenic diabetes mellitus coincides with renal angiotensin dysbalance. *PLoS One*. 2015;10(4):e0121555.

39. Maile LA, Busby WH, Gollahon KA, et al. Blocking ligand occupancy of the alphaVbeta3 integrin inhibits the development of nephropathy in diabetic pigs. *Endocrinology*. 2014;155(12):4665–75.

Figures

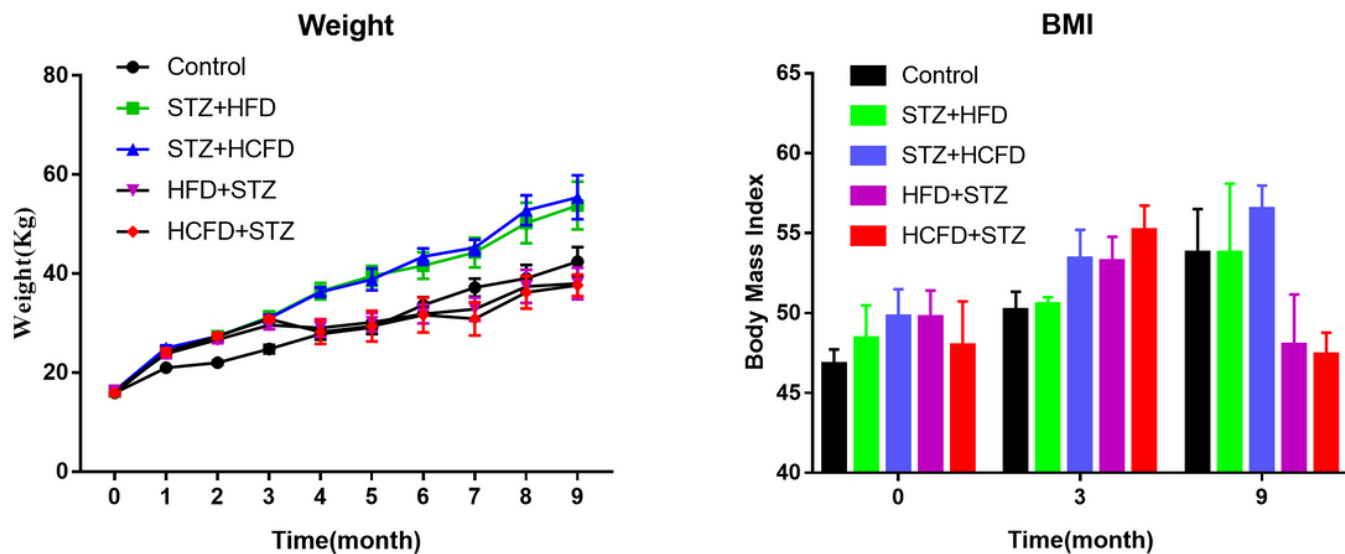


Figure 1

Changes in animal body weight and BMI during the experiment.

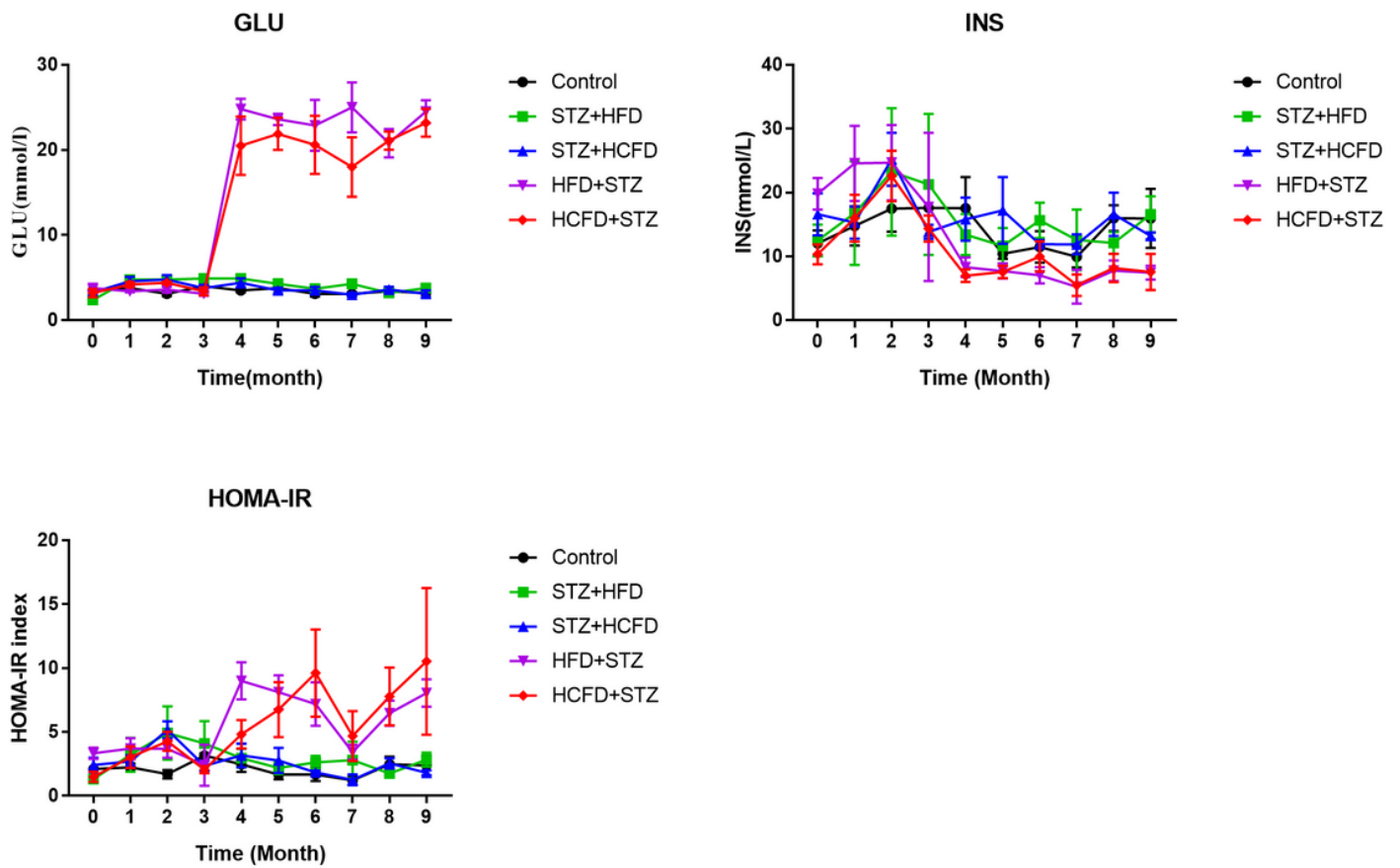


Figure 2

Change of fasting blood glucose (A), fasting insulin (2B), and HOMA-IR Index (C) during the experiment.

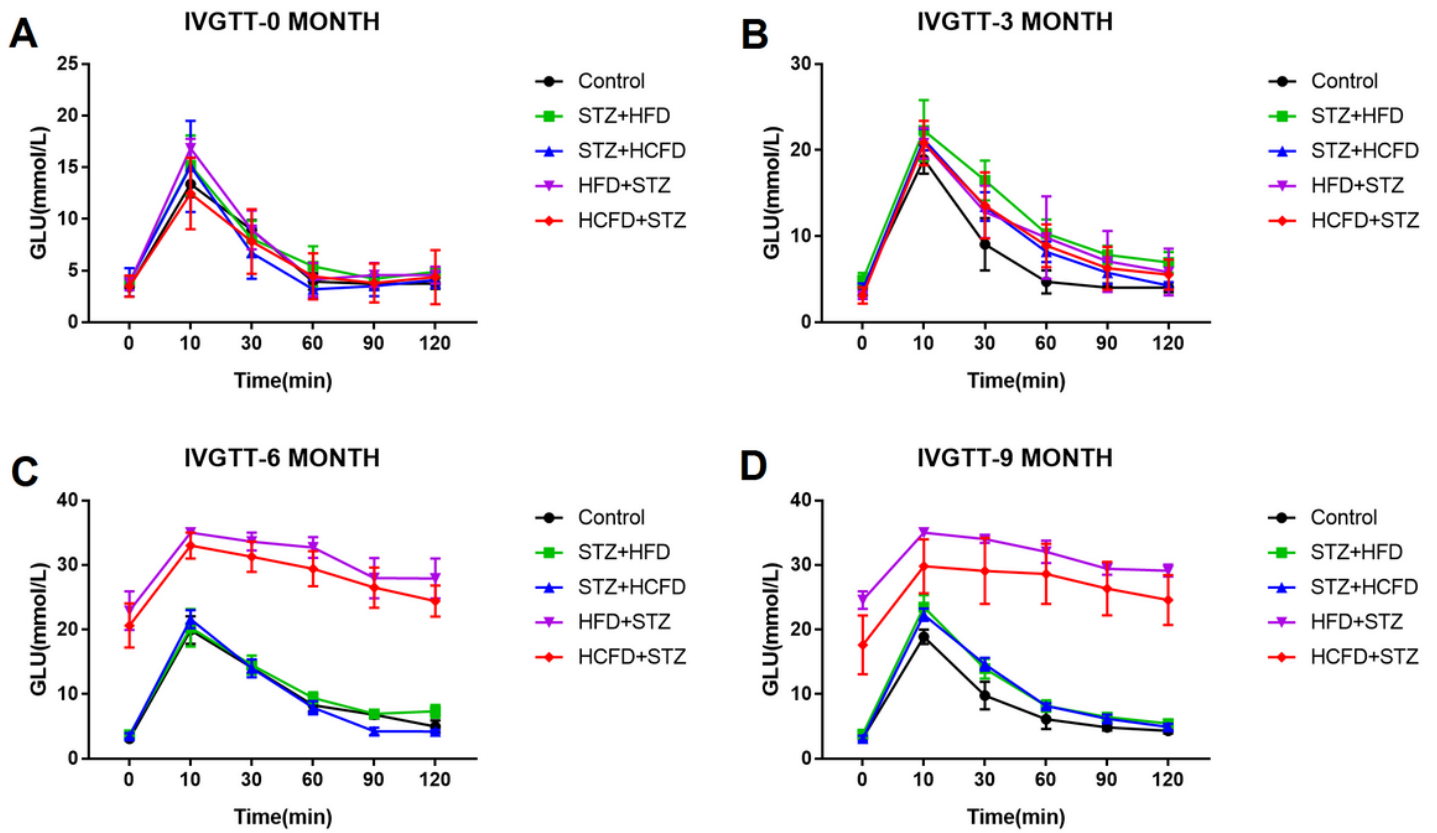


Figure 3

Glucose tolerance test results in a different group on day 1, and at 3, 6, and 9 month

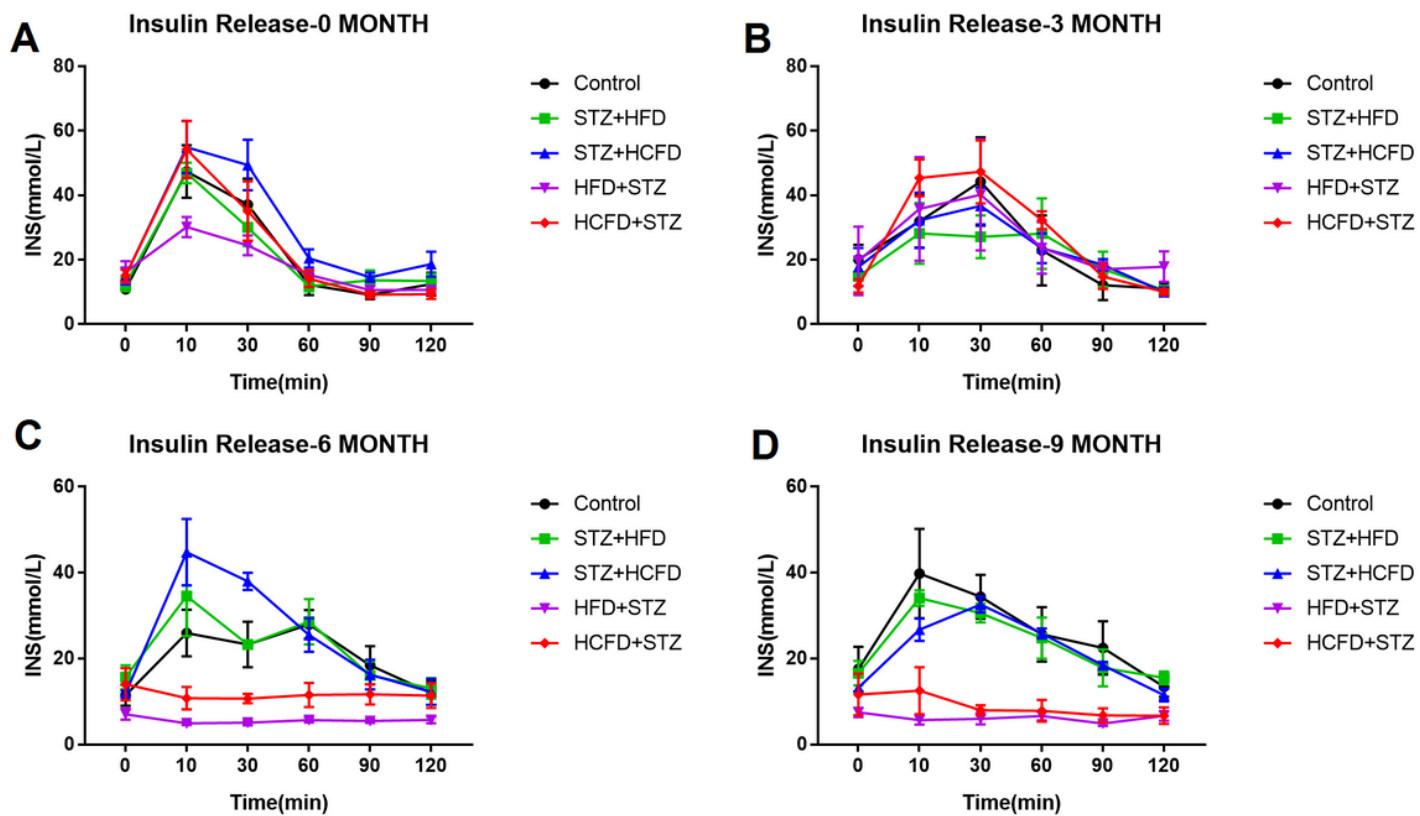


Figure 4

Insulin release test results in a different group on day 1, and at 3, 6, and 9 month

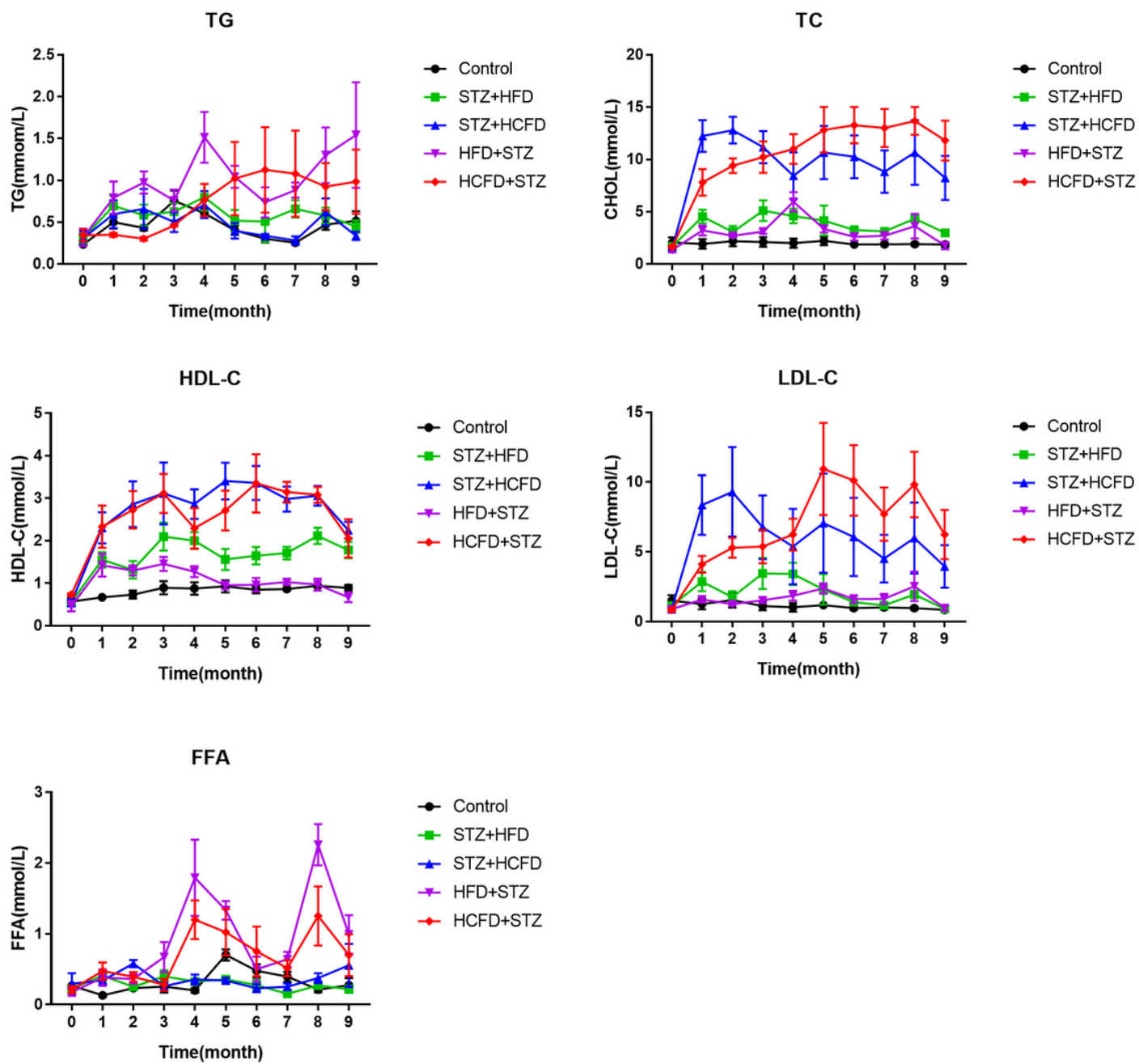


Figure 5

Changes of blood lipid indexes during the experiment. (A)TG; (B) TC; (C)HDL-C; (D) LDL-C; (E) FFA.

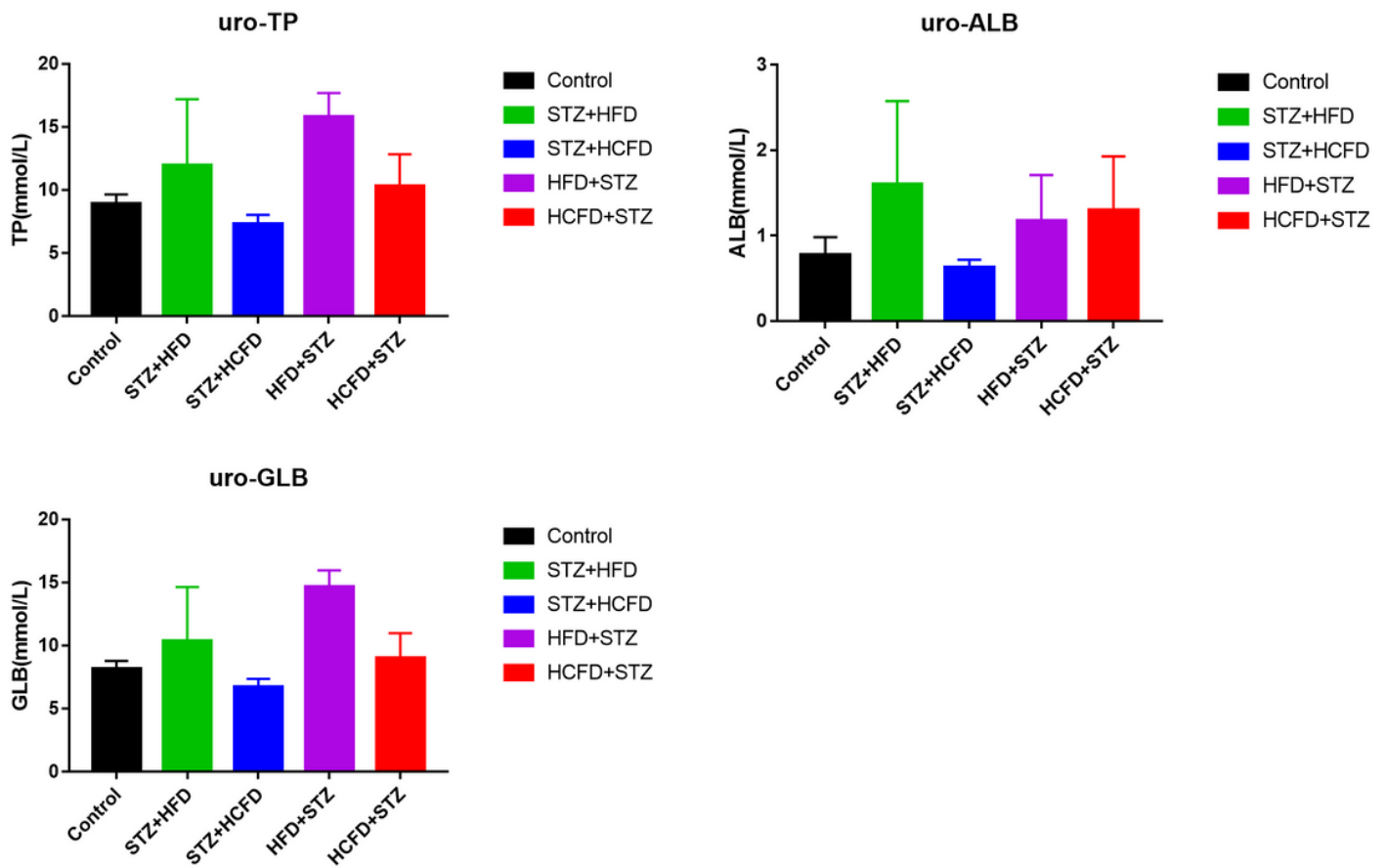


Figure 6

Urine proteins detected nine months after experiment. (A) uro-TP; (B) uro-ALB; (C) uro-GLB.

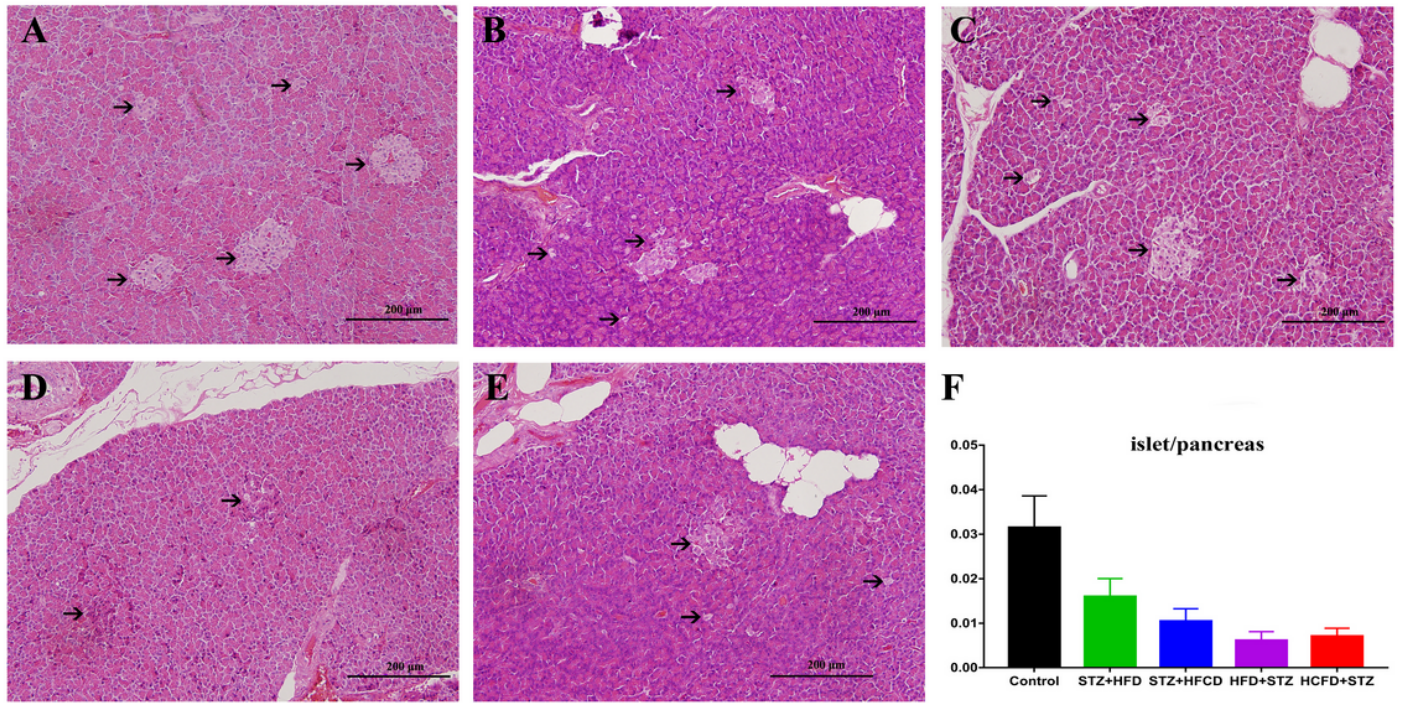


Figure 7

Typical Images of Pancreatic Slices Stained with HE,(→)Point to Islets. (A)Control Group; (B)STZ+HFD Group; (C) STZ+HCFD Group; (D)HFD+STZ Group; (E) HCFD+STZ Group; (F) Islet/Pancreatic Area Ratio of Each Group.

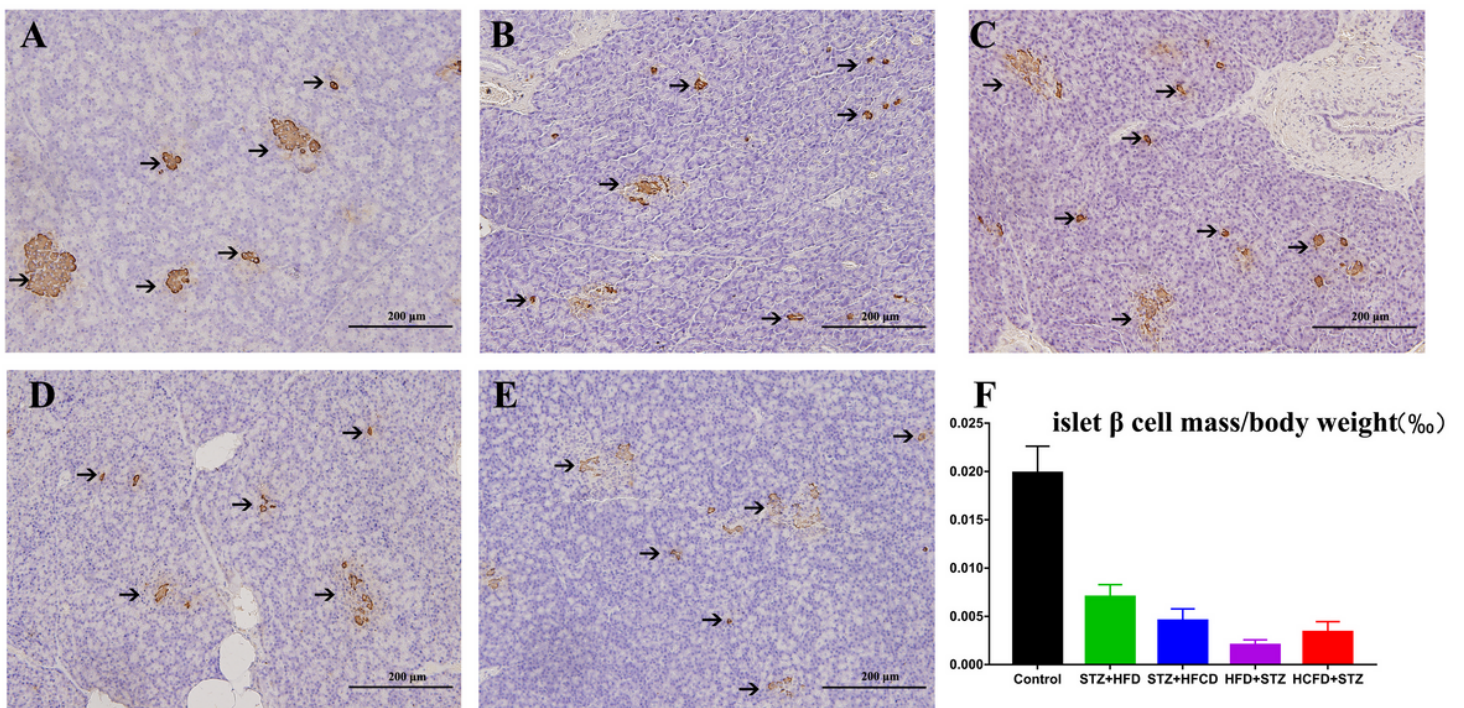


Figure 8

Typical Images of Pancreatic Slices Stained with Insulin Immunohistochemical Staining, (→) Point to Positive Cells. (A) Control Group; (B) STZ+HFD Group; (C) STZ+HCFD Group; (D) HFD+STZ Group; (E) HCFD+STZ Group; (F) Ratio of β Cell Mass/Body Weight of Each Group.

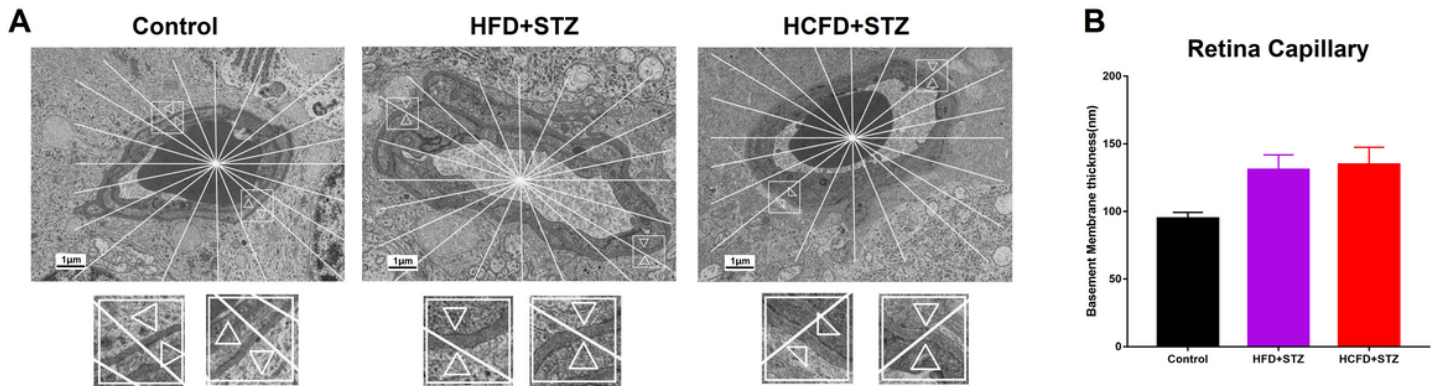


Figure 9

The thickness of the Retinal Capillary Basement Membrane. (A) Typical Picture of Retinal Capillary Ultrastructure and Schematic Diagram of Basement Membrane Thickness Measurement. (B) Measurement Value of Retinal Capillary Basement Membrane Thickness

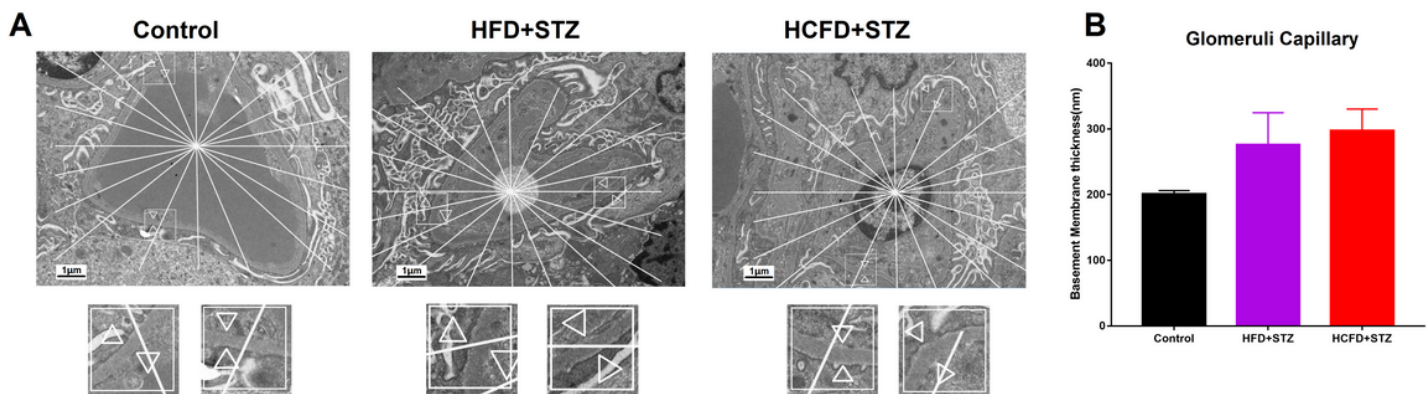


Figure 10

The thickness of the Glomerular Capillary Basement Membrane. (A) Typical Picture of Glomerular Capillary Ultrastructure and Schematic Diagram of Basement Membrane Thickness Measurement; (B) Measurement Value of Glomerular Capillary Basement Membrane Thickness

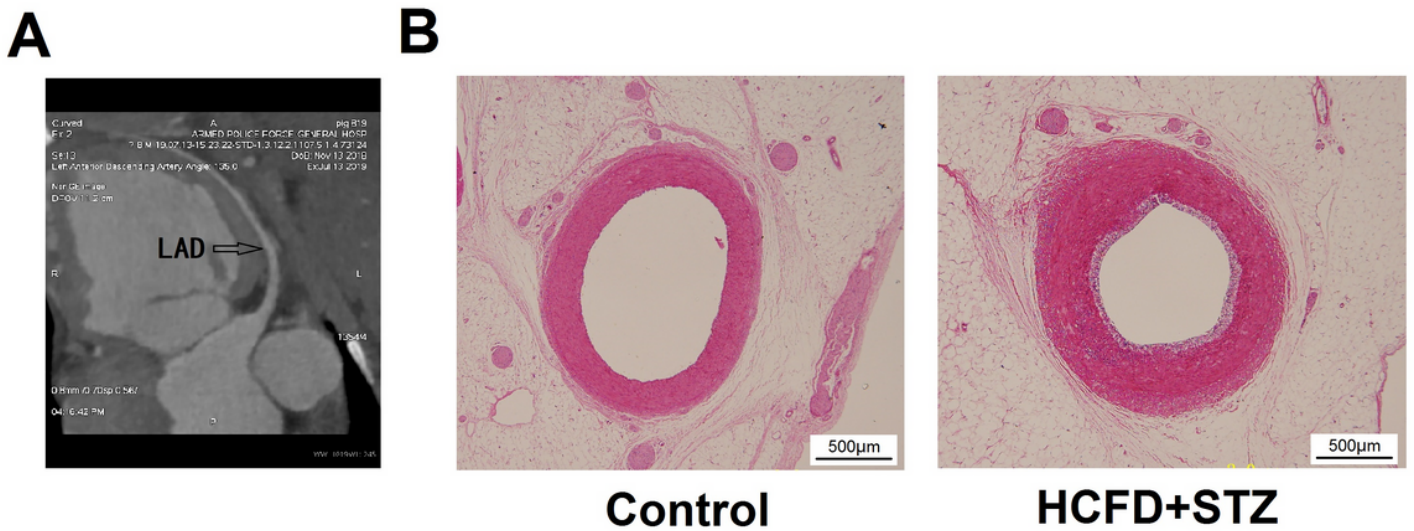


Figure 11

Coronary Artery Examination of Bama Minipigs (A) CT Examination Shows That Coronary Artery Intima Was Intact, Blood Flow Was Unobstructed. (B)The Picture Shows Mild Fatty Streak Lesions in The Coronary Artery Intima Which Was Found in The Anterior Descending Branch of Coronary Artery in One Animal of HCFD + STZ Group. Slide Was Stained with HE.

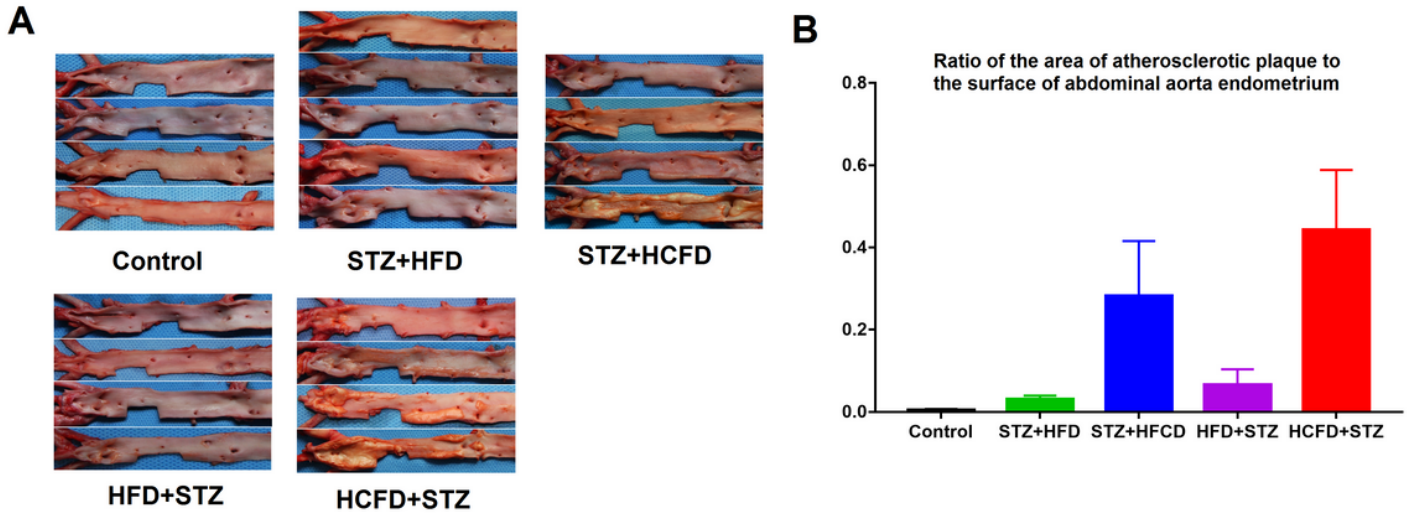


Figure 12

Abdominal Aorta Intima of Animals in Each Group. (A) Longitudinal Incision of Abdominal Aorta of Animals in Each Group, Stained with Oil Red O. (B)Proportion of Abdominal Aortic Plaque Lesion Area to Vascular Intima of Animals in Each Group.